IEEE Transactions ON AUDIO

Volume AU-12 JULY-AUGUST, 1964 Number 4

Published Bimonthly

TABLE OF CONTENTS

CONTRIBUTIONS

AUDIO GROUP

IEEE AUDIO GROUP

The Audio Group is an organization, within the framework of the IEEE, of members with principal professional interest in Audio Technology. All members of the IEEE are eligible for membership in the Group and will receive all Group publications upon payment of an annual fee of $2.00.

IEEE TRANSACTIONS ON AUDIO

Published by the Institute of Electrical and Electronics Engineers, for the Audio Group, at 345 East 47 Street, N.Y. 10017. Responsibility for the contents rests upon the authors, and not upon the IEEE, the Group, or its members. Individual copies, except special issues, may be purchased at the following prices: IEEE members (one copy) $2.25, libraries and colleges $3.25, all others $4.50. Annual subscription price: libraries and colleges $12.75; nonmembers $17.00.

Distributed January, 1965

The Editor's Corner

A NEW INVENTION?

IN THE EDITOR'S CORNER in the May-June, 1959, issue, Edward Logan, Jr. reported the delight of a boy on discovering the acoustical phonograph—a remarkable instrument which had neither tubes nor power cord. We began to wonder what it would really be like if electrical phonographs were commonplace, but no one had thought of trying to make one with a wind-up motor and without electrical amplification until the present day.

An article in one of the technical news magazines might read something like this:

RECORD PLAYER HAS NEITHER TUBES NOR TRANSISTORS

The XYZ Company has announced the development of a mechanically powered portable phonograph. Handwound by a crank, the player has neither power cord nor batteries. Motor power is furnished by a spring capable of storing the required energy indefinitely. An ingenious system of negative mechanical feedback maintains constant speed regardless of spring torque or stylus friction.

The most ingenious feature of the device, however, is the fact that this same spring power produces the sound output—not by running a generator and amplifier, but through direct coupling of the minute stylus vibrations to a diaphragm, which radiates the sound into the air through a built-in horn. Although one might expect the output to register as a faint squeak, volume and fidelity actually are superior to that produced by the typical small transistor portable radio, according to XYZ President James Fisbee.

Mr. Fisbee stated that the phonograph is expected to be a boon to fathers, who have trouble keeping their teenagers supplied with batteries, since the youngsters would provide their own power.

The company also is considering a stereo model, which would have a second horn in a detachable lid connected by eight feet of plastic tubing. However, the monophonic version will be introduced first.

The player will be priced slightly higher than battery-powered, transistorized units.

PETER W. TAPPAN, *Editor*

CALENDAR

1964

Dec. 3–4 Fifteenth Annual Vehicular Communications Symposium, Cleveland, Ohio.

1965

Feb. 3–5 Sixth Winter Convention on Military Electronics, Los Angeles, Calif.

Feb. 17–19 International Solid State Circuits Conference, Philadelphia, Pa.

CALL FOR AUDIO PAPERS

IEEE International Convention, March 22–25, 1965. Send title and abstract by the New Year to:

Frank Comerci
CBS laboratories
Stamford, Conn.

National Electronics Conference, October 25–27, 1965. Contact

James S. Aagaard
Department of Electronic Engineering
Northwestern University
Evanston, Ill.

The IEEE TRANSACTIONS ON AUDIO needs papers, also. See inside back cover.

Charge Transfer Processes in Electrostatic Recording

H. SEIWATZ AND D. E. RICHARDSON, FELLOW, IEEE

Summary—The physical mechanisms responsible for charge transfer between the electrodes and the dielectric tape material of a dc biased electrostatic recording system are discussed. The dominant mechanism for charge transfer is found to be spark discharge in the ambient air. On this basis, a semiquantitative description of the charging process is developed which is in good agreement with the experimental current-voltage characteristics.

I. Introduction

THE OPERATING characteristics of a new system for electrostatic recording have recently been reported.[1] In this system, a pattern of electrical charges corresponding to the signal is produced in a thin insulating tape material by superimposing an ac or dc bias potential on the signal voltage which is applied to the recording electrodes. This paper is concerned with the physical mechanisms responsible for electrode-tape charge transfer in the case of dc bias operation only. Although two pairs of electrodes are normally used in dc bias operation, the basic operating characteristics of the electrostatic recording system are determined by the current-voltage curve for a single pair of electrodes. The purpose of this paper is to discuss the various charge transfer processes which occur when an excellent insulator, such as Mylar,[2] is used as the tape material in a relatively simple system consisting of a single pair of electrodes. The dominant mechanism for charge transfer is found to be spark discharge in the ambient air. On the basis of this mechanism, it is possible to explain semiquantitatively the shape of the current-voltage curve, the magnitude of the minimum bias or threshold voltage, the variation of the threshold voltage with tape thickness, and other experimental observations.

II. Experimental Current-Voltage Characteristics

The basic electrode structure is shown in Fig. 1. A knife edge is in contact with one side of a highly insulating tape and a closely wound helix of fine wire presses against the other side of the tape. When a voltage V is applied to the electrodes and the tape is moving at constant speed, a motional current is observed which is approximately proportional to the capacitance per unit area of the tape, the speed of the tape, and the quantity $(V-V_t)$, where V_t is an empirically determined constant called the threshold voltage. A time variation in V causes a variation in charge density along the length of the tape. The charge density on opposite sides is opposite in polarity and approximately equal in magnitude. The charge distribution in the tape creates an external electric field whose magnitude can be measured by inductive playback.

Current-voltage curves obtained with the same electrode geometry for three thicknesses of type A

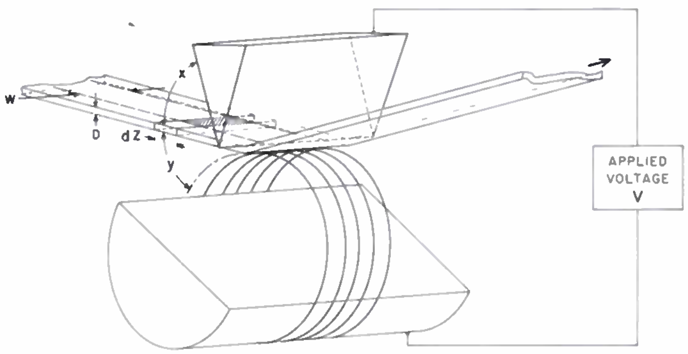

Fig. 1—Basic electrode geometry for electrostatic recording.

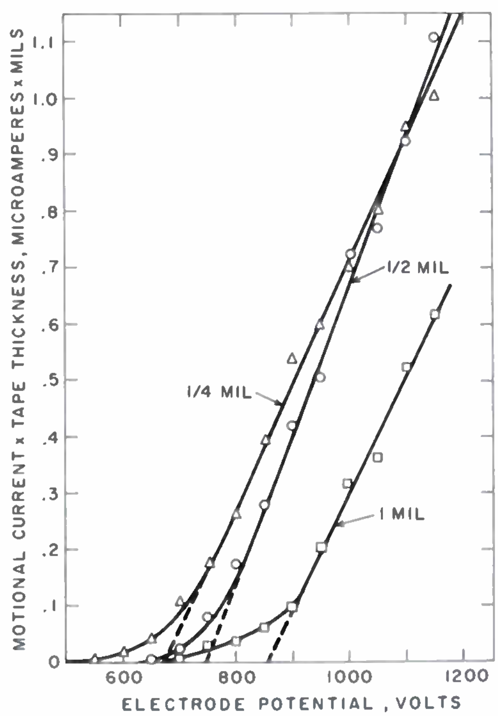

Fig. 2—Motional current multiplied by tape thickness as a function of electrode potential for three thicknesses of Mylar film.

Manuscript received April 24, 1964.
The authors are with the IIT Research Institute, Chicago, Ill.

[1] D. E. Richardson, J. J. Brophy, H. Seiwatz, J. E. Dickens and R. J. Kerr, "A system of electrostatic recording," IRE TRANS. ON AUDIO, vol. AU-10, pp. 95–98; July–August, 1962.

[2] Trademark of E. I. du Pont de Nemours and Co., Inc., Wilmington, Del.

Mylar film are shown in Fig. 2. The threshold voltage in each case is taken to be the intercept on the voltage axis of the straight line which fits the data best at currents within 80 per cent of the current observed at 1150 v. For film thicknesses of $\frac{1}{4}$ mil, $\frac{1}{2}$ mil, and 1 mil, the corresponding threshold voltages from Fig. 2 are 674 v, 748 v, and 855 v with a probable error of ± 5 per cent in each case.

In the vicinity of the threshold voltage, the current-voltage data does not exhibit a linear relationship. The extent of the deviation from linearity in this voltage range depends on the shape of the electrodes and the location of the tape with respect to the electrodes. Small but easily measurable currents are observed at voltages well below the threshold voltage and down to zero volts.

III. Physical Mechanisms of Charge Transfer

The basic fact that charge is transferred between the electrodes and the tape follows directly from the observation of a constant average current between the opposing electrodes when a constant voltage is applied and a tape of uniform thickness moves at constant speed between the electrodes. This observation cannot be explained by any hypothesis which deals only with the internal polarization of the tape material. A workable hypothesis must provide for electrode-tape transfer.

The more prominent possible mechanisms of electrode-tape charge transfer can be placed into four categories; 1) dc conduction, 2) triboelectric effects, 3) high electric field effects, and 4) gas discharge effects. The first category, dc conduction, refers to the steady-state current which is observed when a voltage is applied to the electrodes with the tape stationary. For practical tape materials exhibiting long record life, the dc conduction current is many orders of magnitude smaller than the current observed during electrostatic recording and can be neglected. A triboelectric charging current is observed when the tape is drawn between the electrodes with zero volts applied. The charging current produced by triboelectric effects is small compared to the electrostatic recording current and can be neglected for the purposes of this discussion. However, triboelectric charging is of importance as a source of noise in electrostatic recording and provision must be made for neutralizing such charges in any practical system.[1]

An electric field strength considerably greater than 10^7 v/cm would be expected at the electrode-tape contacts for the geometry shown in Fig. 1 if the tape remained uncharged. Since it is certain that field emission will occur at the negative electrode at such high electric field strengths, charge transfer by this mechanism is definitely a possibility. This hypothesis can be tested by operating the electrostatic recording apparatus in a vacuum. Under these conditions, a charging current is observed but it is smaller than the comparable charging current in air by a factor of about twenty. Evidently, even under the most favorable conditions field emission cannot be of major importance in producing electrode-tape charge transfer.

As the initially uncharged tape approaches the electrodes, favorable conditions for gas discharge must occur in each of the two air gaps between the tape surfaces and the electrodes adjacent to them. Letting p be the air pressure and d the air gap distance along a line of force, all values of pd are possible in each air gap. If the voltage across the air gap exceeds the minimum sparking potential, spark discharges will occur. The quantity of charge which can be transferred by each spark is self-limited since the charge which accumulates at the surface of the tape rapidly reduces the voltage across the air gap to the extinction potential of the spark.

Under these conditions, spark discharge is the dominant mechanism for electrode-tape charge transfer in electrostatic recording. As the discussion in Section IV will show, the tape becomes charged at a distance of about one mil from the points of electrode-tape contact. Thus the electric field strength at the contact points is lower than it would be in a vacuum and the importance of field emission as a mechanism for charge transfer is correspondingly reduced.

IV. Calculation of the Threshold Voltage for an Idealized System

A semiquantitative description of the charging process can readily be developed for the case in which it is assumed that the only mechanism by which a perfectly insulating tape becomes charged is spark discharge in the ambient air. As in Fig. 1, consider a volume element fixed in the tape having dimensions D, W, and dZ, where D is the thickness of the tape, W is the effective width of the tape, and Z is the distance in the direction of tape motion. Since localized sparks occur at irregular intervals along the width of the tape element, the potential at both the top surface and the bottom surface of the tape element varies from point-to-point along the tape width. Neglecting edge effects produced by the finite width of the electrodes, the average potential for the top surface of the tape element is defined as the average of the potential over the area WdZ. Let x be the distance along a line of force from the knife-edge electrode to a point of average potential on the top surface of the tape element. Let y be the corresponding distance between the backing electrode and the bottom surface of the tape element. As the tape element moves toward the electrodes, both x and y decrease monotonically toward zero.

For the case in which $x>y$, sparks will occur first across the gap x, since the dielectric strength of an air gap is smaller for larger gap distances. The charge which is deposited on the top surface of the tape intensifies the field on the opposite side of the tape and thus produces sparks across the gap y. Opposite polarities of charge are deposited on the two surfaces of the tape by this process and the tape dipole moment increases as x decreases. For the case in which $x = y$, the charge density on opposite sides of the tape will be equal in magnitude and opposite in polarity.

For a tape element at a given value of x, the maximum charge density on the top surface of the tape element will occur at a spot where a spark has just been extinguished. The potential difference between that spot and the knife edge electrode will be V_e, the extinction potential of the spark. Under the same conditions, the minimum charge density on the top surface of the tape element will occur at a spot where a spark is about to occur. The potential difference between this spot and the knife-edge electrode will be V_s, the sparking potential of the air. The average charge density on the tape element surface is taken to be that value for which the potential difference V_a between the tape element surface and the electrode is given by

$$V_a = \tfrac{1}{2}(V_e + V_s) \qquad (1)$$

The threshold voltage V_t can be calculated easily for the case in which $x = y$ if the approximation is made that, over the range of x in which spark discharge is possible, the electric field in each air gap is uniform along a line of force. At the bottom surface of the tape, Gauss's law then requires that

$$\sigma = \frac{KK_0V_m}{D} - \frac{K_0V_a}{x} \qquad (2)$$

where σ is the average charge per unit area deposited on the bottom surface of the tape, K is the dielectric constant of the tape material, K_0 is the permittivity of free space, and V_m is the average difference of potential across the tape. Since the voltage V across the electrodes is $2V_a + V_m$, it follows from (2) that

$$V = V_a\left(2 + \frac{D}{Kx}\right) + \frac{\sigma D}{KK_0} \qquad (3)$$

The minimum voltage for sparking V_{tx} for a given value of x is obtained from (3) by extrapolation of the linear relationship between σ and V to $\sigma = 0$, with V_a held constant at the value given by (1). Then

$$V_{tx} = \tfrac{1}{2}(V_e + V_s)\left(2 + \frac{D}{Kx}\right) \qquad (4)$$

Since a tape element encounters all values of x as it moves toward the electrodes, the threshold voltage V_t is the minimum value of V_{tx} with respect to x. According to this calculation, the threshold voltage depends only on the sparking characteristics of the ambient air and the ratio D/K of the tape material.

In order to compute the threshold voltage as a function of tape thickness for a given tape material, it is necessary to determine both V_s and V_e for an air gap between a metal electrode and a dielectric. It has been shown experimentally that the discharge characteristics of air in dielectric voids and metal-to-dielectric gaps are about the same as in metal-to-metal breakdown.[3-5] Accordingly, values for V_s are derived from the Paschen curve data of Meyer[6] for an air gap between metallic electrodes. The determination of V_e by measurements with metallic electrodes is less straightforward because V_e decreases greatly with increasing spark energy. In the present case, values for V_e are derived from measurements made with metallic electrodes in which the spark current is limited by a large series resistance and the electrode capacitance is held to a minimum. Under these conditions, a constant spark extinction voltage of 294 v ±5 per cent is observed for the gap distances of interest at atmospheric pressure. The variation of V_t with tape thickness can then be evaluated numerically for Mylar ($K = 3.2$) by finding, from (4), the minimum value of V_{tx} with respect to x, holding D constant. The result is presented in Fig. 3 for comparison with the experimental values of V_t taken from Fig. 2. The agreement is good.

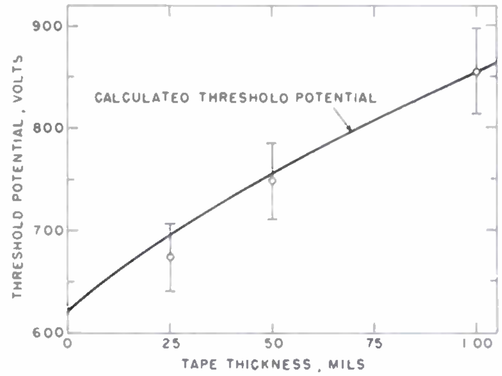

Fig. 3—Comparison of calculated threshold voltages with values from the experimental curves of Fig. 2.

A qualitative extension of the above calculation to the case in which the air gaps are not equal, $x \neq y$, is helpful in explaining how spark discharge can contribute to the recording current at voltages below the calculated threshold voltage shown in Fig. 3. For a given tape element, spark discharge will begin first in the longest

[3] H. C. Hall and R. M. Russek, "Discharge inception and extinction in dielectric voids," *Proc. IEE, II*, vol. 101, pp. 47–54; February, 1954.

[4] M. C. Halleck, "Calculation of corona-starting voltage in air-solid dielectric systems," *Trans. Am. IEE., III*, vol. 75, pp. 211–216; April, 1956.

[5] B. Gross, "Static charges on dielectrics," *Brit. J. Appl. Phys.*, vol. 1, pp. 259–267; October, 1950.

[6] E. Meyer, "Über die Beeinflussung des Funkenpotentials durch ein transversales Magnetfeld," *Ann. d. Physik*, vol. 58, pp. 297–332; March, 1919.

air gap at an electrode voltage which may be almost as low as the minimum sparking potential for a single air gap. The current-voltage characteristic derived for this case is similar to the one derived for equal air gaps in that a linear relationship is predicted at high electrode currents. However, at low electrode currents, it is expected that the curve will be concave upwards and that the electrode voltage at which the spark discharge current begins will be reduced. These qualitative predictions for the low current region of the curve are consistent with the experimental results shown in Fig. 2.

V. Discussion

As the preceding calculation indicates, the basic features of the electrostatic recording current-voltage curve can be explained satisfactorily on the basis that the mechanism for electrode-tape charge transfer is spark discharge in the ambient air. Since the minimum sparking potential in air at atmospheric pressure occurs at a gap spacing of 0.3 mil, the minimum wavelength which can be recorded on the tape must be at least as large. Furthermore, each spark produces a charged spot on the tape whose finite size is a source of noise and an increase in the minimum wavelength.

In order to reduce recording noise, it is desirable to reduce the size of the discrete sparks or to eliminate the sparks altogether in favor of a more uniform gas discharge process. The spark size can be reduced by using a high resistivity electrode to limit the effective capacity which can be discharged by each spark. The use of high frequency bias eliminates the problem of discrete sparks by creating a plasma near the electrodes. The provision of sufficient initial ionization to establish a Townsend discharge will also eliminate sparking.

Acknowledgment

The support of E. I. du Pont de Nemours and Co. is gratefully acknowledged. The authors would like to thank Dr. J. J. Brophy for his encouragement and interest in this work.

The RC Amplifier-Type Active Filter: A Design Method for Optimum Stability

W. R. KUNDERT, MEMBER, IEEE

Summary—The RC amplifier filter has many advantages over its passive RLC counterpart for low-audio frequency or narrow-band applications. The major disadvantage to an active filter has been its sensitivity to component tolerance and drift, particularly where high Q's are involved.

A design method is presented which optimizes transmission stability when the probable "drift" (tolerances, temperature and aging effects, tracking errors) in each circuit parameter is known. Design equations are derived for a group of two-pole networks with external zeros.

Two experimental high-Q filters are discussed including a continuously tunable four-pole filter which has attenuation of 80 db at twice and at one-half center frequency.

Introduction

It has been recognized that the RC amplifier filter has an advantage in size, weight and cost over its passive RLC counterpart for high Q or low-frequency applications. An additional advantage exists when a tunable filter is required since only one element kind, usually the resistors, need be variable. The main disadvantage to the active filter has been its sensitivity to component tolerance and drift. Especially where high Q's are involved, transmission may be extremely sensitive to changes in circuit parameters and the use of such filters is sometimes avoided for this reason.

The RC amplifier filter is usually synthesized as an isolated cascade of two-pole networks. Networks have been contrived[1] to give either internal or external zeros of transmission. The configurations that give transmissions having external zeros are of greatest practical importance since they are used to realize the common transmission forms (Butterworth, Chebyshev, linear phase, etc.). Also, such networks allow some freedom in the selection of circuit constants to achieve a specified transmission. This freedom has been used somewhat arbitrarily[1,2] to simplify design procedure or to minimize the number of different component values needed.

Manuscript presented at the 1964 International Convention; revised manuscript received October 8, 1964.

The author is with the General Radio Company, West Concord, Mass.

[1] R. P. Sallen and E. L. Key, "A practical method of designing RC active filters," IRE Trans. on Circuit Theory, vol. CT-2, pp. 74–85; March, 1955.

[2] A. N. Thiele, "The design of filters using only RC sections and gain stages," *Electronic Engrg.*, pp. 31–36; January, 1956.

This practice may have an adverse affect on the stability of the filter.

The design freedom that exists can be used to minimize errors in the filter if the probable errors in each circuit parameter are known. These errors may be due to temperature drift, component tolerance, aging, and, in a tunable filter, tracking. Depending on the design requirements, one or possibly all sources of error should be taken into account. In any case, there is only one solution of circuit parameters for a given set of parameter error conditions given the restrictions of a specific transmission and minimum error in that transmission. This fact is extremely useful in minimizing cost within the bounds of given performance requirements or in maximizing performance given a restriction on cost. When only maximum performance is of concern, one can have some measure of confidence that it has been achieved.

The Filters

The Isolated Filter

The two-pole filter section of Fig. 1(a) has the transmission

$$\frac{E_2(S)}{E_1(S)} = \frac{\dfrac{K_1K_2}{\tau_1\tau_2}}{S^2 + \dfrac{\tau_2 + (1 - K_1K_2)\tau_1}{\tau_1\tau_2}S + \dfrac{1}{\tau_1\tau_2}} \tag{1}$$

where $\tau_1 = R_1C_1$ and $\tau_2 = R_2C_2$. K_1 and K_2 are considered as ideal voltage amplifiers. Zeros of transmission are fixed by the configuration, at infinity. The poles are defined by the resonant frequency ω_0 and damping ratio δ of the denominator. From (1)

$$\omega_0 = \frac{1}{\sqrt{\tau_1\tau_2}} \tag{2}$$

$$\delta = \sqrt{\frac{\tau_2}{\tau_1}} + (1 - K_1K_2)\sqrt{\frac{\tau_1}{\tau_2}} \tag{3}$$

Inspection of (2) and (3) shows the possible infinite number of values for the circuit constants that can be used. Consider the various sensitivity factors for ω_0 and δ.

For

$$S^{\omega_0} = \frac{\dfrac{\partial\omega_0}{\omega_0}}{\dfrac{\partial\tau_1}{\tau_1}} = \frac{\dfrac{\partial\omega_0}{\omega_0}}{\dfrac{\partial\tau_2}{\tau_2}} = -\frac{1}{2}.$$

There is no possibility of controlling these but they are quite low. For δ, it is convenient to first define

$$\beta = \sqrt{\frac{\tau_2}{\tau_1}} \quad \text{and} \quad K_1K_2 = K$$

ISOLATED TWO-POLE NETWORKS

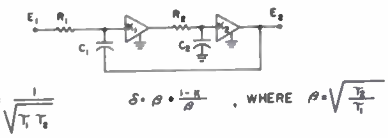

(a)

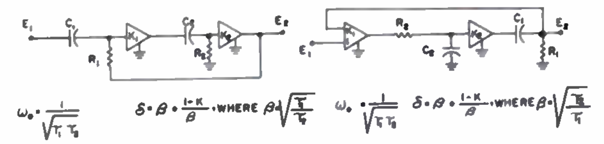

(b) (c)

Fig. 1—(a) Two zeros at ∞. (b) Two zeros at 0. (c) One zero each at 0 and ∞.

Then (3) becomes

$$\delta = \beta + \frac{1 - K}{\beta} \tag{4}$$

Differentiating (4) to find the sensitivity factors yields

$$S_\beta = \frac{\dfrac{\partial\delta}{\delta}}{\dfrac{\partial\beta}{\beta}} = \frac{\beta - (1 - K)\dfrac{1}{\beta}}{\delta} \tag{5}$$

$$S_K = \frac{\dfrac{\partial\delta}{\delta}}{\dfrac{\partial K}{K}} = -\frac{K}{\beta\delta} \tag{6}$$

Apparently it is possible to exert some control over drift in δ. The best choice of parameters will depend on the relative magnitudes of the maximum expected drift in K and β. The total expected drift in δ for the worst case when the effects of drift in K and β are added is given by

$$\left|\frac{d\delta}{\delta}\right| = \left|S_\beta\frac{d\beta}{\beta}\right| + \left|S_K\frac{dK}{K}\right| \tag{7}$$

If a drift ratio

$$r = \frac{\left|\dfrac{dK}{K}\right|}{\left|\dfrac{d\beta}{\beta}\right|}$$

is defined, (7) becomes

$$\left|\frac{d\delta}{\delta}\right| = \left|S_\beta\frac{d\beta}{\beta}\right| + \left|rS_K\frac{d\beta}{\beta}\right| \tag{8}$$

which reduces to

$$\left|\frac{d\delta}{\delta}\right| = [\,|S_\beta| + r|S_K|\,]\left|\frac{d\beta}{\beta}\right| \tag{9}$$

substituting (5) and (6) in (9) gives

$$\left|\frac{d\delta}{\delta}\right| = \left[\left|\frac{\beta-(1-K)\dfrac{1}{\beta}}{\delta}\right| + r\left|\frac{K}{\beta\delta}\right|\right]\left|\frac{d\beta}{\beta}\right| \qquad (10)$$

Eliminating K in (10) by substitution of (4)

$$\left|\frac{d\delta}{\delta}\right| = \left[\left|\frac{2\beta-\delta}{\delta}\right| + r\left|\frac{\beta^2-\delta\beta+1}{\delta\beta}\right|\right]\left|\frac{d\beta}{\beta}\right|$$

For the case when $\delta \leq 2$ and $\beta \geq \delta/2$

$$\left|\frac{d\delta}{\delta}\right| = \left[\frac{2\beta-\delta}{\delta} + r\,\frac{\beta^2-\delta\beta+1}{\delta\beta}\right]\left|\frac{d\beta}{\beta}\right| \qquad (11)$$

$|d\delta/\delta|$ will be a minimum for

$$\frac{d}{d\beta}\left[\frac{2\beta-\delta}{\delta} + r\,\frac{\beta^2-\delta\beta+1}{\delta\beta}\right] = 0$$

which is the case when

$$\beta = \sqrt{\frac{r}{2+r}} \qquad (12)$$

This is a condition for optimum stability. When $\delta \leq 2$ and $\beta < \delta/2$ the same procedure gives no useful solution.

Fig. 2 is a plot of (12) over the range of practical importance while Fig. 3 shows the amplifier gain that is required for various choices of β. Two arbitrary parameter choices have been widely used in similar circuits. One is to set $\beta = 1$ as this allows the use of both equal resistors and equal capacitors; a convenient arrangement. Fig. 2 shows that this solution should be used only when the amplifier gain is much less stable than the time constant ratio (β^2). A second common approach is to set amplifier gain equal to unity, the reasoning here being to allow the simplest amplifier. For small values of δ, the curves show that this choice is best only when the time constant ratio is much less stable than the gain K.

To illustrate the importance of selecting the optimum β, suppose a given filter design requires a section with a damping ratio of 0.1. Suppose furthermore that long term drift in the filter is critical. Within given space and cost limits, it seems possible to use passive components that are likely to age such that $|d\beta/\beta| = 0.005$. An amplifier can be constructed with expected long-term drift $|dK/K| = 0.001$. Then

$$r = \frac{0.001}{0.005} = 0.2 \quad \text{and} \quad \beta_{\text{opt}} = \sqrt{\frac{0.2}{2+0.2}} = 0.302$$

The expected total drift in δ versus β is shown in Fig. 4. The expected drift at β_{opt} is about half that at $\beta = 1$. One may wonder if, in the usual case, it is practical to determine long-term drift in components accurately. Indeed, it is not, but often other more predictable circuit errors will overshadow long-term component drift. In any case, an educated guess is better than selecting components arbitrarily.

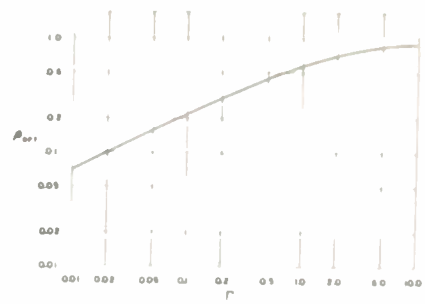

Fig. 2.

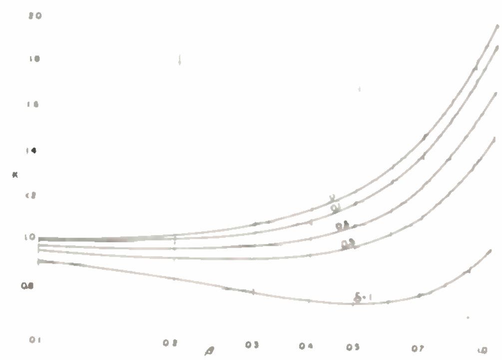

Fig. 3.

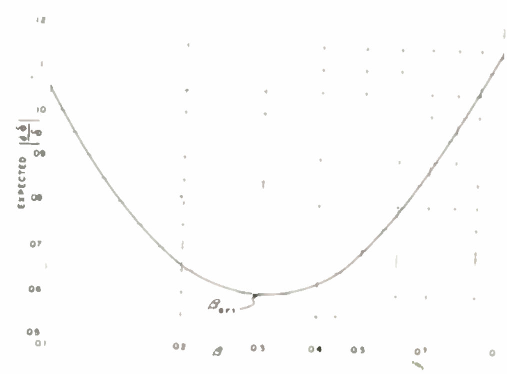

Fig. 4.

The Nonisolated Filter

The circuits shown in Fig. 5 use only a single amplifier. For each circuit

$$\omega_0 = \frac{1}{\sqrt{R_1R_2C_1C_2}}$$

$$\delta = \frac{1}{\rho\gamma} + \frac{\rho}{\gamma} + (1-K)\rho\gamma \qquad (13)$$

where ρ and γ are either resistance or capacitance ratios as shown. Sensitivity factors are found by differentiating (13)

$$S_K = \frac{\dfrac{\partial\delta}{\delta}}{\dfrac{\partial K}{K}} = \frac{-\rho\gamma K}{\delta} \qquad (14)$$

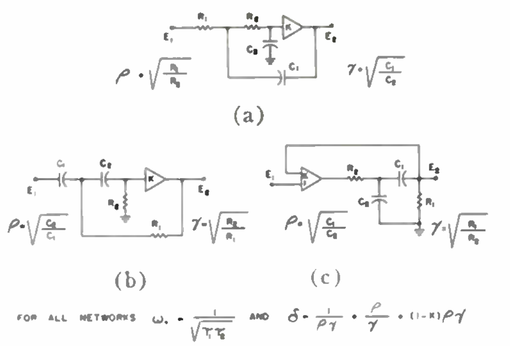

Fig. 5—Three two-pole networks. (a) Two zeros at ∞. (b) Two zeros at 0. (c) One zero each at 0 and ∞.

$$S_\gamma = \frac{\frac{\partial\delta}{\delta}}{\frac{\partial\gamma}{\gamma}} = 1 - \frac{2(1+\rho^2)}{\rho\gamma\delta} \qquad (15)$$

$$S_\rho = \frac{\frac{\partial\delta}{\delta}}{\frac{\partial\rho}{\rho}} = 1 - \frac{2}{\rho\gamma\delta} \qquad (16)$$

Attempts to analyze this type of filter in the same manner as the isolated filter have led to difficulty though study of the sensitivity equations shows that the same general conditions exist. S_γ and S_ρ can be made small but only at the expense of a large S_K. When passive component errors are large compared to amplifier errors, a design should be carried out such that S_K is large and S_γ and S_ρ are small. For the circuit of 5(a), this requires that

$$\frac{R_2C_2}{R_1C_1}$$

be small just as for the isolated filter. However, to achieve the same stability for the nonisolated filter as for the isolated filter, given equal quality components, requires that the resistance ratio R_2/R_1 be made large. This may lead to an extreme spread in component values and the need for an amplifier with higher power gain. For this reason, there appears to be no advantage to the nonisolated filter when a low value of δ is desired.

Stability of R, C, and K

It is interesting, at this point, to speculate as to what limitations might be imposed on the stability of a two-pole filter by available commerical grade components. An amplifier having sufficiently high open-loop gain will have closed-loop gain stability approaching that of the resistive divider that comprises the feedback network. Wire-wound or film resistors are available with temperature coefficient tolerance of ± 20 ppm/°C or better. Long-term drift, also of this order, is realizable. Closed-loop gain drift considerably less than this can be achieved in a series-voltage-feedback amplifier for gain near unity since, under this condition, sensitivity of the feedback factor to changes in the resistors becomes small. Furthermore, a unity-gain amplifier, constructed such that no feedback divider is used, can be made stable without limit.

For the isolated filter, when $K=1$

$$\delta\Big|_{K=1} = \beta$$

$$S_\beta\Big|_{K=1} = 1, \qquad S_K\Big|_{K=1} = -\frac{1}{\beta\delta}$$

For the nonisolated filter, when $K=1$,

$$\delta\Big|_{K=1} = \frac{1}{\rho\delta} + \frac{\rho}{\gamma}$$

$$S_K\Big|_{K=1} = -\frac{\rho\gamma}{\delta} \qquad S_\gamma\Big|_{K=1} = -1$$

$$S_\rho\Big|_{K=1} = \frac{\rho^2-1}{\rho^2+1}$$

For $0<\rho<\infty$, $-1<S_\rho<1$.

Setting $\rho=1$ imposes no restriction on the range of δ. Then

$$S_\rho\Big|_{\substack{K=1\\ \rho=1}} = 0$$

For each type of filter, an infinitely stable unity-gain amplifier allows remarkable performance. Drift in δ is of the same order as drift in the passive components, independent of the value of δ.

Residuals

In practice, it soon becomes evident that component residuals limit the δ stability which can be achieved. To discuss each possible residual in detail would be a difficult if not impossible task which will not be attempted. Some residuals can be reduced to the point where their effect is insignificant. Amplifier-driving-point impedances fall into this category. Others are fixed and must be tolerated. Capacitor loss is of this type. In fact, capacitor dissipation factor is by far the most troublesome residual when a low value of δ is desired.

Fig. 6 shows an isolated filter that includes equivalent shunt conductance for the capacitors C_1 and C_2. It can be shown that the use of unity-gain amplifiers here will limit the minimum value of δ, preventing the extraordinary performance predicted in the preceding section. For this circuit

$$\delta = \frac{\beta(1+R_1G_1)}{\sqrt{1+R_1G_1+R_2G_2}} + \frac{1-K+R_2G_2}{\beta\sqrt{1+R_1G_1+R_2G_2}} \qquad (17)$$

The effect of G_2 is to reduce both R_2 and the gain from the input of K_1 to the input of K_2. An equivalent gain and resistance can be defined to include G_2.

FILTER WITH RESIDUALS G_1 AND G_2

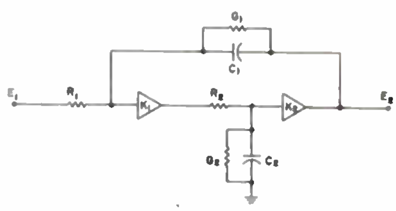

Fig. 6.

$$K' = K \frac{1}{1 + R_2G_2}$$

$$R_2' = \frac{R_2}{1 + R_2G_2} \tag{18}$$

Then (17) becomes

$$\delta = \beta \frac{\sqrt{1 + R_1G_1}}{\sqrt{1 + R_2G_2}} + \frac{1 - K'}{\beta \dfrac{\sqrt{1 + R_1G_1}}{\sqrt{1 + R_2G_2}}} \tag{19}$$

From (19), an equivalent β can be defined as

$$\beta' = \beta \frac{\sqrt{1 + R_1G_1}}{\sqrt{1 + R_2G_2}} \tag{20}$$

To minimize drift in K' due to drift in the dissipation factor of C_2, R_2G_2 should be as small as possible. However, for a given capacitor type, the product $R_1R_2G_1G_2$ is fixed.

$$R_1R_2G_1G_2 = D^2$$

where D is the dissipation factor of the capacitors. A small R_2G_2 is possible only at the expense of a large R_1G_1 and inspection of (20) shows that this combination is undesirable from the standpoint of minimizing drift in β'. It should be noted that

$$\beta = \sqrt{\frac{R_2C_2}{R_1C_1}} = \sqrt{\frac{R_2G_2}{R_1G_1}}$$

so when a value is selected for β, the drift contributed to K' and β' by drift in G_1 and G_2 is fixed.

Though no straightforward method of handling capacitor loss has been found, several observations can be made based on the preceding equations and experimental evidence.

1) Dissipation factor and drift in dissipation factor becomes critical only for low values of δ ($\delta < 0.01$). In these cases, low-loss mica or polystyrene capacitors are desirable. For higher values of δ, paper or mylar dielectrics may be adequate.

2) There is little to be gained in making K more stable than the quantity $(1 + R_2G_2)$.

3) The extremely low values for β, suggested when K is at or very near unity should be avoided. Generally, β should be no less than 0.1.

Two High Q Filters

A Tunable Filter

A tunable narrow-band audio analyzer presents one of the best applications for an RC active filter. The filter circuit for such an analyzer is shown in Fig. 7. Resistors have been chosen as the variable element to keep impedance-level compatible with transistor circuitry and to minimize size. The filter covers the entire audio range in several bands selected by switching capacitors (not shown). A bandwidth of one per cent is obtained with a synchronously tuned cascade of two sections. One section has a Q of 80 ($\delta = 1/80$) and the other a Q of 40 ($\delta = 1/40$). This spreading of Q's reduces the problem of frequency tracking between the sections though there is some sacrifice in flatness of the filter response curve near the peak. The interchanged placement of R's and C's for the two sections results in a symmetrical over-all response with an ultimate attenuation rate of 12 db/per octave at low and high frequencies (see Fig. 8).

Tracking errors that cause variation in damping ratio as the filter is tuned account for the largest circuit error. Potentiometer tolerance allows a peak-to-peak, variation in R_2/R_1 of 0.5 per cent. Another error associated with tuning is a slight change in apparent gain due to the loading effect of the input impedance of the amplifiers on the RC networks. Three-transistor amplifiers provide a ratio of input-to-output impedance of the order of 10^8 and gain drift versus temperature better than 10 ppm/°C.

A value for β of approximately 0.3 has been found to give the best results for tracking over the entire audio range. Equations (5) and (6) show, for the section that has $Q = 80$,

$$S_\beta = 49$$

$$S_K = 280.$$

Measured variation in peak response and bandwidth due to tracking errors is, for the over-all filter, ±0.6 db. Over-all temperature coefficient for gain and bandwith is less than 0.01 db/°C.

A Two-Pole Filter With Q = 1000

A filter with a Q of 1000 has been constructed using a circuit similar to that in the high Q section of the tunable filter. The amplifiers, each constructed with three high-gain transistors, have temperature coefficients less than 1 ppm/°C. The capacitors are polystyrene units with dissipation factor less than 10^{-4} and nominal temperature coefficient of capacitance of +140 ppm/°C. The resistors have a possible range in temperature coefficient of ±20 ppm/°C. Since the amplifiers appeared to be ten-to-twenty times more stable than β, a value for β of 0.2 was chosen and from (5) and (6) gives

$$S_\beta = 399 \qquad S_K = 5150$$

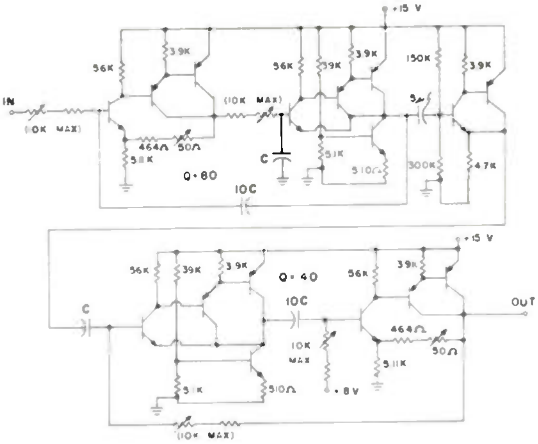

Fig. 7—Tunable narrow-band filter.

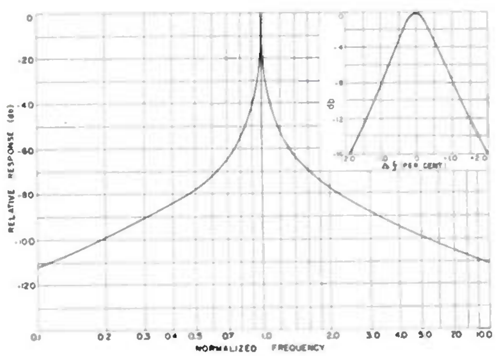

Fig. 8—Tunable narrow-band filter.

The measured temperature coefficient for Q is -0.08 db/°C which is near what would be predicted from component drift.

Conclusion

The following important conclusions have been drawn from the results of this investigation:

1) For many audio applications, the RC amplifier filter can be made more stable than its RLC counterpart, with equal expenditure.

2) In the circuits shown, and most likely in all such circuits, a trade-off exists between sensitivity factors for gain (S_K) and passive components (S_β).

3) An amplifier with gain near unity can easily be constructed with much greater stability than that of readily available passive components. For this reason, a high sensitivity factor for gain usually can be tolerated and allows a low sensitivity factor for passive components.

4) The dissipation factor and drift in dissipation factor of the capacitors used place an upper limit on Q stability. It is probably impossible for circuit Q to exceed the Q of the capacitors without also exceeding the drift in Q of the capacitors.

Acknowledgment

The author gratefully acknowledges the interest and guidance, particularly in the mathematical analysis, of A. Peterson of the General Radio Company.

Magnetic Tape Recording Materials

C. D. MEE, SENIOR MEMBER, IEEE

Summary—The design criteria for magnetic recording tapes are considered with respect to the desirable physical and magnetic characteristics for high resolution recording systems; in particular, the magnetic properties of the universally used iron oxide powders are compared with possible competitive permanent magnet materials. The properties of oxide and metal powders and of metallic thin films are compared, and the possibility of their future use in high output high resolution tapes is also assessed in this paper.

SINCE MAGNETIC tape has undergone intensive development during the past 20 years, it seems appropriate to consider the design of currently manufactured tape and to speculate on its future development. The general construction of most tapes consists of a single magnetic coating adhering to a flexible plastic carrier; with very few exceptions, the magnetic material used is gamma ferric oxide in the form of needle-shaped particles. There is some variety in the plastic base material, including polyester films, polyvinyl chloride, and cellulose acetate. The polyester film is now used extensively in high grade high resolution applications.

This paper discusses the magnetic materials used in tape and considers the possible future competition to ferric oxide powders. Although it is concerned specifically with magnetic tapes, other forms of magnetic recording, for instance with disks or drums, have many similar requirements. Both saturation recording, as used for digital and frequency modulated (FM) signals, and linear recording are considered with regard to the desirable magnetic properties of the tape. Storage problems and reproduction efficiency also are discussed to establish the over-all tape design criteria, possible new magnetic materials for tape are reviewed, and examples of their comparable linear recording performance are given.

Tape Design Criteria

Physical Requirements

The essential function of the recording medium in conventional magnetic tape systems is to produce at the surface of the reproducing head a magnetic field whose amplitude has the same time variation as that occurring during the recording process. To allow continuous physical contact between the tape and the recording or reproducing head, it is important that the tape surface be smooth and relatively soft, thus ensuring maximum interaction between the magnetic materials in the tape and head. Because of the finite thickness of the magnetic layer, magnetic poles inside the tape contribute a relatively small part of the tape surface field. This loss may be minimized by using, as the recording medium, a very thin layer of a high remanent magnetization material. This, in turn, makes a high packing density of magnetic material desirable, which conflicts with the required pliable nature of the coating for good head-to-tape contact.

Up to the present time, the general physical requirements for magnetic tape have been met most adequately with a magnetic layer consisting of a fine magnetic powder dispersed in a plastic binder and coated onto a thin plastic tape. All-metal tapes have certain restricted uses, where only long wavelengths are encountered, and where the gain in maximum tape surface field overrides the loss caused by imperfect contact with the heads. A possible successful tape design may arise from using thin metallic layers on a plastic base material to combine physical flexibility and large surface fields.

The general tape construction, consisting of a magnetic coating on a nonmagnetic carrier, also has the advantage that each layer may be optimized separately to fulfill its allotted function. The desirable features of good long-term physical stability, uniformity, flexibility, and low density are all aimed at in the base material; the coating is designed to yield optimum magnetic properties, along with a suitable physical surface permitting constant transportation velocity past the head and intimate contact over the whole tape width. Both base and coating should be as thin as possible to achieve a maximum volume density of information in a recording; this also provides good tape flexibility. If equivalent physical properties can be maintained in thin base layers, the limiting factor will be the magnetic printing effect between adjacent layers in the wound tape. As the magnetic coating thickness is reduced, an additional problem arises since mechanical flaws in the coating cause a relatively greater undesirable amplitude modulation of the reproduced signal.

Recording Resolution and Efficiency

In the recording process, using a conventional gapped ring head, the magnetic layer of the tape is subjected momentarily to a magnetic field whose maximum amplitude is sufficient to cause irreversible magnetization. At the same time, the field direction experienced by an element of tape rotates from perpendicular to the layer to parallel with it as the tape approaches the maximum field zone, and vice versa as it leaves this zone. Under optimum working conditions, the field amplitude falls

Manuscript reprinted from IEEE TRANS. ON COMMUNICATIONS AND ELECTRONICS, vol. CE-83, pp. 399–408, July, 1964. A portion of this paper has been taken by the author from his book, *The Physics of Magnetic Recording*, North Holland Publishing Co.; their permission to use this material is appreciated.

The author is with the Thomas J. Watson Research Center, IBM Corporation, Yorktown Heights, N. Y.

below that required to produce irreversible magnetization in the region near the gap edge where the field, seen by an element of tape, is changing at a maximum rate. It is in this region, at the trailing edge, that recording effectively takes place. High-sensitivity and high-resolution recording require that a maximum magnetization be achieved in the rapidly diminishing trailing-edge field. In considering the recording resolution, it would seem that the best results would be obtained by minimizing the effect of the perpendicular component of the applied field. The resolution will also be improved when the dispersion of critical fields for irreversible magnetization is minimized in the magnetic layer. This condition is evidenced by a remanent magnetization characteristic which approaches a step function, and by a linear anhysteretic magnetization characteristic. (The anhysteretic magnetization process refers here to a simultaneously applied ac and dc field; the ac field, initially of sufficient amplitude to saturate the material, is reduced to zero while the dc field remains constant.)

When recording with ac bias, the magnetization process taking place is basically a modification of the anhysteretic magnetization process. There are a number of differences between anhysteretic magnetization and ac bias recording, which include the simultaneous reduction of ac and dc fields, rotation of the fields, and variation of maximum applied field in different parts of the coating. Despite these complications, however, the linearity of the anhysteretic magnetization curve is closely related to the recording characteristic.

In pulse recording, the tape is magnetized to saturation by the signal field from the recording head and information is imparted to the recording signal by reversing its direction. The reproducing-head voltage must be a maximum when the tape magnetization reversals are detected. The reproduced voltage is determined by the averaged product of the reproducing-head field function, the slope of the remanent magnetization curve $\delta I_x''/\delta H_{xw}$, and the slope of the recording-head field function $\delta H_{xw}/\delta x_t$. Optimum recording resolution will thus be obtained if the maxima of the remanent magnetization curve slope and of the recording-head field coincide, and if these curves are sharply peaked; these functions are plotted in Fig. 1(a) for a finite recording-head gap length [1]. Their product is the derivative of the tape magnetization with respect to distance along the tape $\delta I_x''/\delta x_t$. However, as shown in Fig. 1(b), this function spreads considerably with increased depth in the coating, illustrating the increased average magnetization transition zone length for the whole coating. Furthermore, on taking account of the reproducing-head field function, the reproduced pulse width will be increased somewhat. Nevertheless, it is found that measured pulse widths are even wider than predicted by this analysis. To account for this, self-demagnetization effects in the magnetization transition region must be considered.

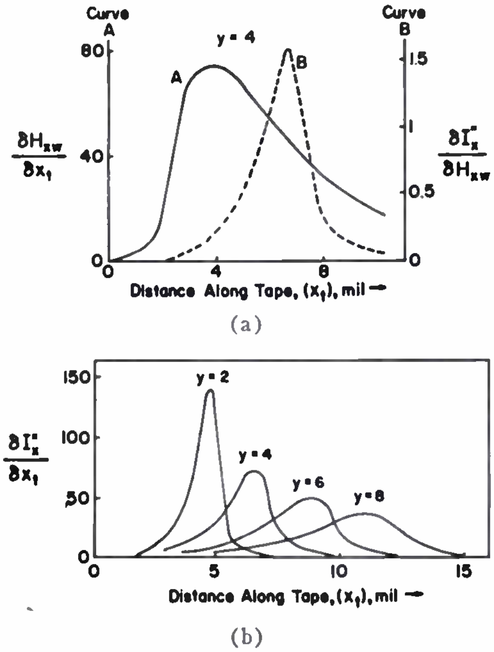

Fig. 1—Nonreturn to zero step function recording. (a) Recording head trailing edge field (curve A) and magnetization curve slope (curve B), y = head to tape spacing (mils); gap length = 7 mils. (b) Recorded magnetization slopes.

Thin coatings are seen to be advantageous for pulse recording. If a high-remanent magnetization material is used to offset the reduction of coating thickness, it would be necessary to increase the coercivity and to maintain a rectangular demagnetization characteristic to minimize demagnetization losses. It has been shown that, even for the ratios of remanent magnetization to coercive force found in iron oxide tapes, the demagnetization effects cause significant increases in the magnetization transition zone [2]. Improved pulse recording resolution may be expected, therefore, from higher coercivity and squarer loop tape material.

Storage Problems

From the time that a tape leaves the vicinity of the high-permeability pole pieces of the recording head, a variety of circumstances can arise which tend to destroy the magnetization acquired during recording. As the tape leaves the recording head, the magnetized particles in the tape no longer have their intrinsic demagnetizing fields shunted by the poles of the recording head. Consequently, these fields increase inside the particles, causing reversible and irreversible demagnetization losses. When the recorded tape then is wound on the take-up reel and stored, the magnetization will readjust itself to the lowest energy condition for this environment. Readjustment will consist of self-demagnetization and magnetization effects, caused by external fields and by fields from adjacent tape layers, respectively.

The question of optimizing the magnetic field at the surface of the tape has been considered so far only from the point of view of obtaining a maximum surface field for reproduction. With respect to the printing of signals between layers of a wound reel of recorded tape, a large field is undesirable. Alternatively, the magnetic material of the tape should be insensitive to remagnetization by small dc fields, which may be accompanied by other energies such as temperature rise or external ac fields. The basic phenomenon involved is magnetic viscosity caused by thermal fluctuations. When a magnetic field is applied to a material consisting of single-domain particles, the resulting change in magnetization may take a finite time as a result of relaxation effects. For the same reason, when the field is removed, the magnetization may gradually decrease with time. The magnitude of this phenomenon depends critically on the particle volume and the temperature. In general, when the volume is small enough to be in the range where single-domain properties give way to superparamagnetic properties, applied fields smaller than those necessary to switch the single-domain particles can, in time, produce further magnetization in the field direction. Low susceptibility to unwanted printing effects during tape storage would then seem to be obtained, if the particle volume distribution can be restricted. The trend towards high-resolution tapes on which shorter wavelengths are recorded reduces the severity of the print-through problem, since the printing field from adjacent recorded layers in a tape is reduced when the ratio of recorded wavelength to layer separation is small.

Reproduction Efficiency

During the reproducing process, the recorded tape is transported in the vicinity of the high-permeability pole pieces of the reproducing head. Each magnetic particle in the tape has an associated external demagnetizing field. These fields produce the greatest magnetization of the soft magnetic core of the reproducing head when they are positioned in the region of the head gap. There is also a partial recovery of reversible demagnetization loss at this time. If the tape is demagnetized, the particle fields are randomly directed and give rise to random magnetization of the core and a consequent noise voltage across the core winding. On the other hand, if the tape is recorded, the particle fields become ordered in direction, producing a head core magnetization proportional to the number of unidirectionally magnetized particles.

Although the magnetization achieved in recording is not uniform with depth at short wavelengths because of the reduction of recording resolution with separation from the recording head, this is possibly not a major factor in determining the reproducing head flux. This viewpoint is based on the conjecture that the wavelength-dependent thickness and separation losses in reproduction are more severe than the corresponding reduction of recorded magnetization with depth in the coating on recording. It is important to design a tape so that a maximum intensity of magnetization can be transported in close proximity with the reproducing-head gap: this requires a very thin magnetic layer, with high-saturation magnetization and a smooth yielding surface to allow good contact with the transducer.

The reproduced noise of an unrecorded tape can be attributed to the inhomogeneity of the magnetic layer. In conventional powder tapes, the effective particle size determines the background noise level. This size is influenced by both the degree of spatial dispersion of the particles and the individual particle volume. The optimum particle size is the smallest compatible with magnetic stability. Another noise component, modulation noise, which occurs on reproducing a magnetized tape, is a function of the magnetization level and can be considerably greater than the background noise. Experimentally, the major source of modulation noise appears to be spurious amplitude modulation of the recorded signal caused by variations in the physical and magnetic properties of the tape [3]. Nonuniformities in the tape surface appear to be a major cause of this type of noise [4]. Physical and magnetic nonuniformities in the coating and unevenness in the backing material can also contribute to the magnetization-dependent noise.

Permanent Magnet Materials for Tape

The specification of the desirable magnetic properties for a magnetic tape material obtained from the analyses of the recording and reproducing processes is now considered with respect to the theoretical mechanisms of magnetization in permanent magnet materials. A number of suitable materials may be considered competively.

As has been described, a highly nonlinear magnetization characteristic must be developed in a magnetic material for tape recording. This will yield a high sensitivity to recording signals in the presence of a suitable bias, and low sensitivity to magnetization change by spurious fields after recording. An irreversible magnetization process controlled by some critical energy is, therefore, required. Such a process is obtained in materials exhibiting single-domain behavior. Bulk materials achieve magnetization changes by domain-wall motion, essentially a linear process, which can be avoided by producing very small regions of the magnetic material in which the formation of domain boundaries is energetically unfavorable. Magnetization reversal then takes place by some characteristic mode of rotation of the magnetization vector. The magnetization characteristic is controlled by the internal anisotropies of the magnetic regions which oppose the rotation of the magnetization vector towards the field direction. The controlling anisotropy should be so oriented that, after saturating the material, a minimum magnetization change occurs on removing the field. Furthermore, on increasing the applied field in the opposite direction to the magnetization, minimum magnetization change should occur until a critical field is reached, where maximum irreversible magnetization in a small field range should take place.

At first sight, there appear to be several magnetic

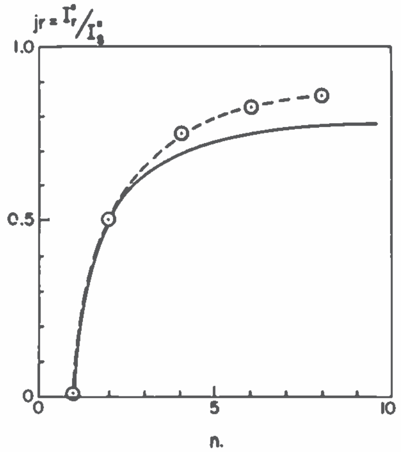

Fig. 2—Reduced remanent magnetization vs number of easy directions (n); ⊙- - -⊙ spatial distribution; —— planar distribution.

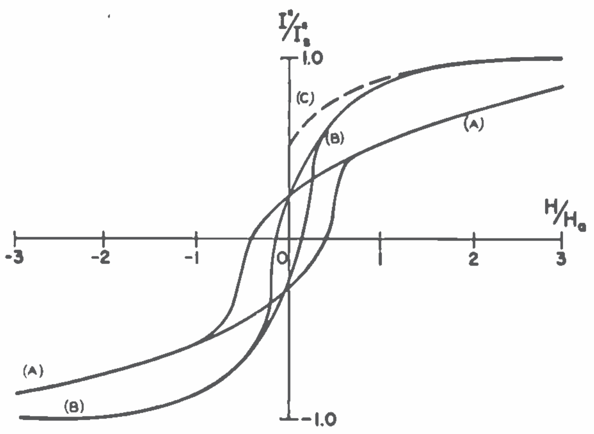

Fig. 3—Hysteresis loop for mixed magnetization modes. (A) Equal quantities of single-domain and multidomain particles. (B) Equal quantities of single-domain and paramagnetic particles. (C) Single-domain particles only.

anisotropies which could be harnessed to yield the desirable form of hysteretic magnetic properties. The shape anisotropy in small needle-shaped particles produces the most satisfactory tape material, since it can be closely controlled to give good uniformity of properties and is reasonably stable with respect to temperature fluctuations. However, if this anisotropy is unoriented, a theoretical ratio of remanence to saturation of only 0.5 is obtained. Fig. 2 shows how the ratio of remanence to saturation increases with the number of easy directions of magnetization for both spatial and planar distributions [5]. An inherently higher ratio would, therefore, be obtained in materials with a dominant cubic crystal anisotropy having six or eight easy directions of magnetization. The disadvantage of such materials for tape is that crystal anisotropy is strongly temperature-dependent, leading to instability of the recorded signal. Stress anisotropy is caused by the change of crystal anisotropy associated with an applied stress. The relationship between crystal and stress anisotropies leads to similar formulas for the energies with which they are associated. Apart from the question of the stability of such an induced anisotropy, it would appear to be difficult to achieve any high degree of uniformity in a product relying on this type of anisotropy. Another induced anisotropy may be obtained by magnetic annealing of certain materials but, again, the thermal stability of such materials is inferior to those controlled by shape anisotropy alone.

In any practical material it is impossible to produce only one form of anisotropy, and sometimes both shape and crystal anisotropy are significant. As will be shown, it is possible that the advantages of both types of anisotropy might be combined. Another important constraint is on the distribution of particle sizes. The desirable single-domain behavior is obtained only in a certain particle size range. Smaller and larger particles outside this range exhibit superparamagnetic and multidomain behavior, respectively. If these are mixed with single-domain particles, the remanent magnetization is reduced compared to that obtained from single-domain particles alone [6], as shown in Fig. 3. The particle size range for single-domain behavior varies from one material to another. The best results will be obtained in a material with a large single-domain range.

The desirable property that all regions in the material have the same critical field for irreversible magnetization imposes restrictions on the shape and homogeneity, as well as the size, of the single-domain regions. Furthermore, when these regions are placed close together, as in a practical tape, the effective critical field is determined by the local field, because of the presence of neighboring magnetized regions, as well as by the intrinsic critical field of the region. Uniformity of the local field will depend on that of the spatial distribution of the magnetized regions.

The search for suitable magnetic tape materials thus seems to center around the requirement that an easy and stable direction of magnetization exist near the applied field direction for each single-domain region, and that the critical fields for irreversible magnetization change be the same for all such regions. The properties of suitable magnetic materials are reviewed next in the light of these magnetic requirements.

Additional selectivity is imposed by the physical requirements of a tape recording system. A smooth-surfaced flexible thin magnetic layer is required in order to give good contact between the tape and the recording and reproducing transducers. Although magnetic alloys containing single-domain ferromagnetic precipitates have been produced in wire and strip form, it is not possible to optimize these physical requirements while retaining sufficient thickness for the over-all mechanical strength required in a tape. Thin films of permanent magnet alloys deposited onto a plastic base material appear to be much more promising in this respect. Some examples of recent developments will be described. By far the most successful method of producing single-domain regions has been the development of techniques for making uniform acicular fine particles. Good magnetic properties can be combined with the required physical properties by preparing uniform dispersions of such powders in a plastic binder. It is in the formulation and application of such a coating that present-day tapes differ. Magnetic materials in the form of powders and thin films are therefore considered in this paper. Present-day tapes utilize the ferrimagnetic oxide γFe_2O_3. Oxides, metals, and alloys will be discussed also.

Permanent Magnetic Oxide Powders

Typical values for the magnetic and physical properties of some magnetic oxide powders suitable for use in magnetic tape are listed in Table I, headed by the ferric oxide powder presently used. The acicular particles [7] have a typical length-to-width ratio of 5 to 1. In this case, the associated shape anisotropy considerably exceeds the crystal anisotropy of this material. Some idea of the theoretical limits of these anisotropies may be obtained by comparing the anisotropy fields $H_a = 2\pi I_s = 2500$ oersteds and $H_a = 2K_1/I_s = 235$ oersteds, which correspond to an infinite cylinder and a single crystal, respectively. Although these limits are not reached in practice, the dominance of shape anisotropy in these powders is confirmed. The intrinsic coercive force H_c, saturation magnetization I_s'', and remanent magnetization I_r'' refer, where possible, to values expected in tapes. I_r''/I_s'' is assumed to be 0.75 for oriented acicular particles, and a volume packing density of 40 per cent is assumed for powders. By modifying the preparation techniques, it is possible to produce acicular particles an order of magnitude smaller than those listed. These have similar hysteresis properties to the larger particles. However, they have the possible advantage of lower background noise level in recording, and the possible hazard of increased instability with respect to external fields and temperature fluctuations.

Nonacicular particles of γFe_2O_3 or magnetite (Fe_3O_4), with a diameter of about 0.2 micron, may be produced by precipitating the hydroxide from a ferrous salt solution followed by controlled oxidation. The properties of both oxides are listed in Table I, where it can be seen that Fe_3O_4 has a slightly larger specific saturation magnetization than γFe_2O_3 ($\sigma_s = 92$ and 80, respectively). For these, the shape anisotropy is reduced to the same order of magnitude as the crystal anisotropy, giving a low value of coercive force for both the γFe_2O_3 and Fe_3O_4 particles, thereby entailing a large self-demagnetization loss. The resulting remanent magnetization is only about one-third of the corresponding value for oriented acicular particles, which show little loss of this type.

Thus, for iron oxide powders, it appears that the best properties are obtained in oriented acicular particles. Since magnetite has the higher saturation magnetization, it is expected that it would be preferred. However, it is less stable than ferric oxide and exhibits magnetic accommodation effects which make it difficult to erase permanently a recording made on this material. Hence, oriented acicular particles of ferric oxide are preferred. The magnetic and physical properties of these particles will be compared with other oxides and metals which might be competitive for magnetic tape use.

A possible alternative to acicular iron oxide powders exists in oxides with sufficiently high cubic crystal anisotropy to enable this to be the dominant anisotropy in a tape powder. In this case, the particles may be isotropic in shape, and very small particles, not requiring orientation, can give the desired rectangular hysteresis loop with $I_r''/I_s'' \approx 0.7$. This approach has been used commercially for magnetic tapes [16] by the addition of cobalt ions to cubic iron oxide particles about 0.1 μ in size. Cobalt-doped iron oxide may be prepared by a method similar to that used for nonacicular iron oxide with the addition of cobalt sulfate in the precipitating solution [17], [18]. Cobalt concentrations above 10 per cent of the total metal ions would give coercivities in excess of 1000 oersteds because of the increase in crystal anisotropy. Problems in recording and erasing such magnetically hard material occur.

TABLE I

PHYSICAL AND MAGNETIC PROPERTIES OF SOME PERMANENT MAGNET OXIDE POWDERS

Material	Composition	Physical Properties				Magnetic Properties							
		Crystal Structure	Density (ρ')	Length a(Micron)	Width b(Micron)	H_c	σ_s (Gauss-Cm³/Gm)	I_s'' (Gauss)	I_r'' (Gauss)	H_{at}* (Oersteds)	K_1[1] (Erg/Cm³)	H_a (Oersteds)	T_c(C)
Iron oxide[−10]	γFe_2O_3	Inverse spinel	4.98	1.0	0.2	250	80	160	120§	2,000	0.047	2,500**	675
	Fe_3O_4			0.2	0.2	90	80	160	44‖		0.047	235††	675
Cobalt-iron oxide[11]	$CoFe_2O_4$		5.21	0.2	0.2	115	92	192	52‖	245	0.11	460††	585
	$Co_xFe_{3-x}O_4$†		5.29			4,200	80	170	120‡‡	1,400	2.5	12,000††	520
Barium ferrite[10,12]	$BaFe_{12}O_{19}$	Hexagonal close packed	5.0	0.08	0.08	640	73	146	100‡‡	1,300	1.0	5,500††	
Barium-iron oxide + titanium-cobalt[10]	$BaCo_\delta Ti_\delta$.		5.3	1.0	0.1	4,000	72	148	112§	17,500	3.0	17,000††	450
	$Fe_{12-2\delta}O_{19}$‡		5.34	1.0	0.1	1,900	60	128	96§		1.3	8,200††	
Lead ferrite[13]	$Pb_{1.6}Fe_{11.6}O_{19}$		5.5			500	49	110	82§				
Chromium oxide[14]	CrO_2+Sb	Tetragonal		1.0	0.1	380	90						130
Manganese ferrite[10]	$MnFe_2O_4$	Inverse spinel	5.0				80	160				(100)††	300
Nickel ferrite[15]	$NiFe_2O_4$	Inverse spinel	5.33	0.06	0.06	123	49	105				412††	585

* H_{at} is the estimated anisotropy field at 150 C.
† $x = 0.15$.
‡ $\delta = 0.5$.
§ Estimated value for partially oriented particles $I_r''/I_s'' = 0.75$; assumed volume packing factor = 0.4.
‖ $I_r''/I_s'' = 0.27$.
** $H_a = 2\pi I_s$.
†† $H_a = 2K_1/I_s$.
‡‡ $I_r/I_s = 0.7$.

The magnetic characteristics for particles of pure cobalt ferrite ($CoFe_2O_4$) and for iron oxide doped with 5-atomic-per cent cobalt ($Co_xFe_{3-x}O_4$) are shown in Table I. $CoFe_2O_4$ is too hard magnetically to be considered for conventional magnetic tape use, but has been included in the table to illustrate the exceptionally high anisotropy it attains. For the lower cobalt-content powder, small particles of 800 A (Angstrom units) may be produced with a specific saturation magnetization some 10 per cent lower than γFe_2O_3 or $CoFe_2O_4$, but with adequate coercivity for tape with dominant control by crystal anisotropy. This produces a powder with a similar remanent magnetization to the acicular iron oxide sample, but with the advantages of isotropic properties (thus avoiding particle orientation problems), and also with a very small particle size which should lead to tapes with a low background noise. However, the temperature stability of coercivity is poor since the properties are controlled by crystal anisotropy. As can be seen from the table, the effective anisotropy field H_{at} falls to 24 per cent of its initial value when the powder is heated to 150°C. Some stabilization may be achieved by magnetic annealing [19], but the hazard of the magnetization instability in these materials restricts their application in magnetic recording.

Although it is impossible to avoid the temperature variation of crystal anisotropy in ferrites, it is possible to achieve thermal stability of remanent magnetization in some hexagonal ferrites like barium ferrite ($BaFe_{12}O_{19}$), where the temperature variations of K_1 and I_s are similar and the anisotropy field $H_a=2K_1/I_s$ varies little over the temperature range of interest. Small platelet-shaped particles of $BaFe_{12}O_{19}$ may be produced which exhibit single-domain behavior [20]. However, the very high crystal anisotropy results in coercive forces which are much too high to be practical. Even in the somewhat larger particles listed in Table I the high coercive force is prohibitive for tape use. The crystal anisotropy of uniaxially anisotropic hexagonal ferrites may be reduced by replacing some of the ferric ions by equal amounts of divalent cobalt and tetravalent titanium ions. For instance, the crystal anisotropy may be reduced to 40 per cent of the value for $BaFe_{12}O_{19}$ while the saturation magnetization falls by only 17 per cent [21], as indicated in the table. Although this value is still very large by normal tape standards, such a material might find limited use for special applications requiring high permanence of recordings.

Another very interesting set of hexagonal ferrite materials exhibits lower coercive force than $BaFe_{12}O_{19}$ because of the development of easy directions of magnetization in the plane perpendicular to the hexagonal c axis; then the c axis itself becomes a difficult direction [22], [23]. These materials contain additional divalent ions, such as cobalt, and have six easy directions of magnetization in the basal plane. For small platelet-shaped particles, with easy axes in the plane of the plate, it would be possible to produce a magnetic tape with the plates parallel to the tape plane, giving easy magnetization in the plane of the tape ($I_r''/I_s''=0.75$, in Fig. 2). It would then be difficult to magnetize such a tape perpendicular to the tape plane, a condition which leads to high-resolution recording.

In addition to barium ferrite powders, somewhat similar results are obtained for hexagonal ferrites containing strontium or lead [24], and the saturation magnetization may be increased further by adding a few per cent of SiO_2 or Bi_2O_3. The magnetic properties expected of oriented lead ferrite particles are given in Table I.

A few other ferrites also may be mentioned; in addition to the iron and cobalt ferrites already considered, manganese, nickel, copper, magnesium, and lithium ferrites have simple spinel structures. The first two, which have specific saturation magnetizations approaching those of iron and cobalt ferrites ($\sigma_s=80$ and 50, respectively), are listed in Table I. Manganese ferrite, which has the largest saturation magnetization at low temperatures, has a low Curie point, which is not conducive to stable properties around room temperature. Although nickel ferrites are of some possible interest, the low values of I_s, and even lower values for copper, magnesium, and lithium ferrites, militate against competing them with iron oxides. Chromium dioxide, which has a specific saturation magnetization in the range 80–100 gauss-cm³/gm (gauss-centimeters cubed per gram), may be prepared in fine powder form, and has been considered for use in magnetic tapes [25]. The magnetic properties of these powders are also listed in Table I. It has been shown that the acicular particles are single crystals with the tetragonal axes parallel to the long axes of the particles. Magnetic properties somewhat superior to those of iron oxides are achieved at room temperature. A possible disadvantage of this material is its rather low Curie point.

Permanent Magnet Metal and Alloy Powders

From the preceding review of permanent magnet oxide powders, it appears that the possible improvements over the existing iron oxide powders are concerned both with particles having higher and multiaxial anisotropies and with smaller particle sizes. Metal and alloy powders, on the other hand, have higher intrinsic magnetization, and thus offer the advantage of high-output tapes. Moreover, techniques have been developed for depositing metals directly onto plastic base materials, yielding the possibility of very thin film tapes. For the sake of completeness, the magnetic properties of some "homogeneous" metallic tapes will also be mentioned, although they have severe physical limitations which restrict their use to relatively long-wavelength recording applications.

The physical and magnetic properties of metals and alloys in the form of powders and thin films are listed in Table II, where the alloy compositions are listed by per cent of weight. Here it is seen that saturation mag-

TABLE II

PHYSICAL AND MAGNETIC PROPERTIES OF SOME METALS AND ALLOYS IN POWDER AND FILM FORM

Material	Composition	Physical Properties					Magnetic Properties							
		Crystal Structure	Form	Density ρ'	Length a(Micron)	Width, b(Micron)	H_c (Oersteds)	σ_s (Gauss-Cm³/Gm)	I_s'' (Gauss)	I_r'' (Gauss)	H_{at} (Oersteds)	K_1[1] (Ergs/Cm³)	H_a (Oersteds)	$T_c(C)$
Iron[28]		Body-centered cubic	Powder	7.88	0.04	0.015	825	218	680	460	9,800	0.4	10,000‖	770
			Thin film	7.88			400	218	1,700‡	1,350‡				770
Cobalt[28]		Hexagonal close packed	Powder	8.9	0.04	0.015	2,100††	157	560		2,000	4.1	5,500	1,120
Nickel[28]		Face-centered cubic	Powder	8.9				54	194		90	−0.05	206	358
Iron-cobalt	60% Fe, 40% Co	Body-centered cubic	Powder	8.1	0.1	0.02	1,075	235	750	565†	11,800	0.04	12,000‖	1,000**
Cobalt-nickel	82% Co, 18% Ni	Hexagonal close packed	Thin film	8.9			250	143	1,230	800				
Cobalt-phosphorus[29]	98% Co, 2% P*	Hexagonal	Thin film	8.9	2-Micron layer		400	73	650	440				
Cobalt-nickel-phosphorus[30]	75% Co, 23% Ni, 2% P*	Hexagonal	Thin film	8.9			750	95	840	630				
Iron-cobalt-nickel[31]	55% Fe, 5% Ni, 40% Co, 5% Ni	Body-centered cubic	Powder		0.1	0.05	760		314	239				
Iron-nickel-chromium[32]	76% Fe, 12% Ni, 12% Cr	Body-centered cubic	Thin film				250		160	120				100
	74% Fe, 8% Ni, 18% Cr	Face-centered cubic	Thin film				200			240				
Vicalloy II (vanadium-iron-cobalt)[33]	13% V, 35% Fe, 52% Co	Body-centered cubic	Thin film	8.2			500			730§				
Cunife I (copper-nickel-iron)[33]	60% Cu, 20% Ni, 20% Fe	Face-centered cubic	Thin film	8.1			590			450				
Cunife II	50% Cu, 20% Ni, 2.5% Co, 27.5% Fe	Face-centered cubic	Thin film	8.6			260			580§				
Cunico I (copper-nickel-cobalt)[33]	50% Cu, 21% Ni, 29% Co	Face-centered cubic	Thin film	8.3			700			275				
Cunico II	35% Cu, 24% Ni, 41% Co	Face-centered	Thin film	8.3			450			420				

* Estimated nominal phosphorus content.
† Estimated for partially oriented particles $I_r''/I_s''=0.75$; packing factor $=0.4$.
‡ I_r'', I_s'' are theoretical values.
§ Directional properties.
‖ $H_a=2\pi I_s$.
** Virtual T_c.
†† Random orientation 76 degrees Kelvin.

netizations of iron and cobalt powders, diluted to 40 per cent by volume for a tape coating, are 680 and 560 gauss, respectively, whereas all the oxides listed in Table I have tape saturation magnetizations of less than 200. Nickel powder, on the other hand, has properties not unlike those obtained in γFe_2O_3. Thus, the metals iron and cobalt, and their alloys with each other and with nickel and other elements, may theoretically yield remanent magnetizations up to four times greater than oxide powders.

Table II shows that the crystal anisotropy is some ten times greater for iron than for γFe_2O_3 and the saturation magnetization rather more than four times greater. Thus, the anisotropy field will be about 500 oersteds, leading to $I_r''/H_c \approx 1$. This ratio is considered too high to avoid demagnetization losses. On the other hand, the theoretical anisotropy field, for anisotropy controlled iron particles, is $2\pi I_s$ $(=10{,}000$ oersteds), assuming coherent rotation processes. These do not occur in acicular iron particles, however, which change their magnetization by an incoherent mechanism, probably fanning. Consequently, maximum coercivities around 1000 oersteds are obtainable in practical shape anisotropy controlled iron particles. Single-domain metal particles generally are smaller than the oxide particles now used in tapes. This has been shown to result in a lower background noise level in comparison with similar, but larger, particles.

There are numerous methods for preparing fine metal powders. One very successful method for producing acicular particles employs electrodeposition in mercury [34], in which particles about 150 Å in diameter and length-to-width ratios of up to 10 to 1 are formed. The magnetic properties of typical particles are listed in Table II for a length-to-width ratio of 3 to 1 and a moderate degree of orientation, $I_r''/I_s''=0.65$. Iron-cobalt alloy particles may be produced by the same method. These have the advantage of higher saturation magnetization than either iron or cobalt, and, since shape anisotropy is dominant, they have a correspondingly higher coercivity. The magnetic characteristics of elongated particles of a 60–40 iron-cobalt alloy, listed in Table II, show the expected increase of H_c and I_s''.

Metal oxalates have been used as the starting material for the preparation of fine particles of metals, alloys, metal oxides, and ferrites [35]. Reduction of the oxalates to the corresponding metal or alloy may be carried out by heating in a hydrogen atmosphere to a temperature high enough to effect decomposition, but low enough to avoid sintering. Binary alloy powders of iron-cobalt have been produced successfully by this method, and also ternary alloys of the iron-cobalt-nickel system [36], [37]. Typical magnetic properties for 55 per cent Fe–40 per cent Co–5 per cent Ni are shown in Table II for 0.1-micron-long acicular particles. It can be seen that, at the present stage of development, this method has not produced the maximum magnetization expected from such alloys. This may result from the use of a lower packing density than the 40 per cent figure assumed for the other metal powders. Nevertheless, the magnetic properties of metal and alloy powders, given in Table II, indicate that at least a threefold increase in remanent magnetization may be obtained over that presently obtainable in oxides. Moreover, suitable coercivities may be developed to avoid self-demagnetization effects. The advantages in a magnetic tape are probably best realized by producing very thin layers of metal powder tape, which considerably reduce the recording and reproducing losses associated with the coating thickness, and improve both the efficiency and resolution of the recording process. Finally, the tape noise associated with particle size effects is reduced.

Metal Tapes

The advantages of metal and alloy powder tapes may possibly be realized also in metal thin films in which a homogeneous ductile magnetic layer is produced directly rather than by mixing powders with a plastic binder. Of course, the inherent advantage of averaging out variations in magnetic properties is lost in any direct method of producing the magnetic layer. Nevertheless, the technology for production of uniform thin films has advanced in recent years. Unfortunately, little information on the recording performance of thin film tapes has been published, although the magnetic properties achieved indicate that they represent serious potential competition for high-resolution tapes.

All-metal wires and tapes preceded the modern metal-plastic base combination. Since the requirements for magnetic tape are a combination of magnetic hardness and physical softness, it is not easy to produce satisfactory results for all-metal tapes. However, some magnetic alloys of iron-cobalt, nickel-iron-cobalt, and nickel-cobalt form ductile products when alloyed with copper or vanadium (V), which may be rolled to thin tapes suitable for magnetic recording when very high resolution is not a major requirement. Some of these alloys with the trade names Vicalloy, Cunife, and Cunico are listed in Table II. Iron-nickel-chromium alloy, or magnetic stainless steel, also falls into this category and has been used for wire recording. However, all of these materials suffer from physical rigidity, even in the form of thin tapes or wires, leading to imperfect contact with the recording-reproducing transducers, and to consequent separation losses.

In forming a magnetic thin film layer directly on a plastic base, it would seem that all of the techniques for producing soft thin films for memory elements have possible application to magnetic tapes. Electrodeposited cobalt-nickel has been used as the magnetic recording medium for metal tapes and disks. For these alloys, a hexagonal structure is obtained for more than 72 per cent by weight of cobalt, and large values of saturation magnetization can be achieved in the deposited layer (Table II). It is found that a coercive force of approximately 250 oersteds is obtained in films a few microns thick. The ratio of remanent magnetization to coercive force is about three, which is rather high to avoid self-demagnetization losses. Higher coercivities up to 500 oersteds have been reported for cobalt-nickel electrodeposits where high *p*H in the bath is maintained [38].

The coercivity of Co-Ni alloys may also be increased if the electrodeposition conditions are adjusted so that lamellated structured deposit is formed [39] introducing considerable shape anisotropy. The resulting coercive force can exceed 1000 oersteds. However, this effect is achieved at the expense of reducing the saturation magnetization of the layer, and there must be sufficient porosity to achieve single-domain lamellae magnetically isolated from their neighbors; the method used is the combination of electroless and electrolytic deposition [30]. Typical magnetic properties for this alloy are listed in Table II under Co-Ni-P (phosphorus), and it is seen that the coercive force and saturation magnetization are increased by factors of three and five, respectively, when compared to oxide powder tapes. Thus, for the same tape flux (or long-wavelength output) the coating thickness may be reduced by a factor of five, say to 2 microns. As the short wavelength response depends on the intensity of magnetization rather than on the total tape flux, an increase of five times would then be obtained, compared to iron oxide tapes.

Another interesting property of thin plated layers of Co-Ni-P is that the high value of coercivity and high ratio I_r''/I_s'' are not dependent on the direction of measurement [40]. The desirable magnetic properties for recording are thus obtained without introducing orientation of the controlling anisotropy. Somewhat reduced magnetization and coercive force values are obtained on plating Co-P in the same manner [29]. The plating may be done on metal bases, as described, or on a plastic base previously coated with a conducting substrate. Cobalt has also been plated onto Mylar by an electroless process in which reduction is achieved in the presence of hypophosphite ions [41]. Typical samples of the latter product have a saturation magnetization of 8000 gauss and a coercive force of 360 oersteds. Such tapes, with a coating about 1.0 micron thick, show similar nonreturn-to-zero pulse packing and pulse width to that obtained with iron oxide computer tapes, together with a slightly lower output.

Permanent magnet behavior has been obtained in very thin layers of electrolytically deposited iron without the lamella structure [27]. However, it is necessary to reduce the iron thickness considerably to achieve high coercivity. Interleaving with a nonmagnetic conductor would be a possible method to build a sufficiently thick layer for recording purposes. In this case the 100 per cent volume packing factor assumed for the saturation magnetization value in Table II is too high. Perhaps 50 per cent of this value is nearer the practical value. Less success has been obtained in attempts to evaporate thin permanently magnetic metal layers, and the properties of the bulk material are obtained for

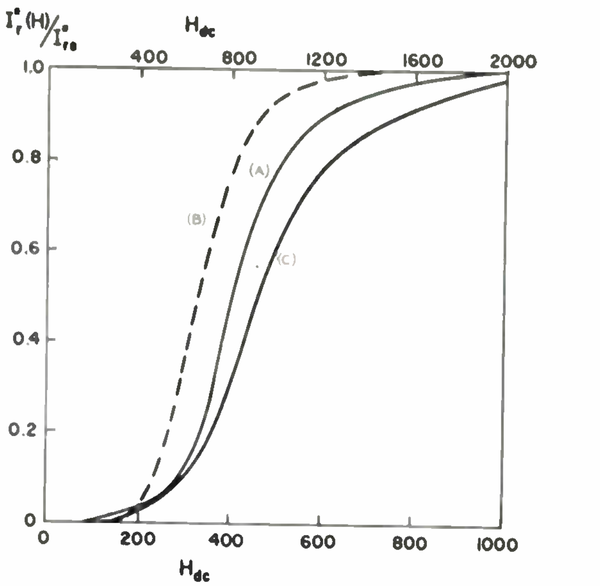

Fig. 4—Relative tape remanent magnetization curves; $I_r''(H)/I_{ro}''$; H_{dc} in oersteds. (A) Cobalt-doped iron oxide powder. (B) Oriented gamma ferric oxide powder. (C) Iron-cobalt-nickel alloy powder.

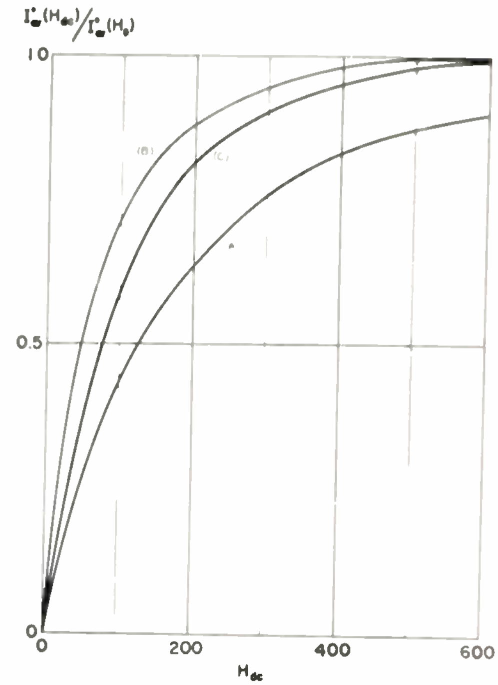

Fig. 5—Relative anhysteretic remanent magnetization curves, H_{dc} oersteds. (A) Cobalt-doped iron oxide powder. (B) Oriented gamma ferric oxide powder. (C) Iron-cobalt-nickel alloy powder.

small thicknesses. Evaporated cobalt layers have been reported with a coercivity of 40 oersteds for a thickness less than 1 micron [42]. Elsewhere higher coercivities have been obtained and values up to 2810 oersteds at 77° Kelvin have been reported in cobalt films evaporated in the presence of a magnetic field [43]. It can be expected that evaporation techniques will be developed further, leading to controllable permanent magnet behavior suitable for magnetic tape application.

To summarize the present state of metal tape development, it seems that the optimum magnetic and physical properties can be obtained in thin layers of alloys and metals deposited onto a plastic base; very smooth surfaces can be formed which promise high-resolution recording. It remains to be seen if the physical and magnetic quality control of such tapes can be maintained at the level of powder tapes in production today.

Recording Performance of Tapes

The recording performance of the promising possible tape materials will depend on the physical as well as the magnetic properties of the manufactured tape. New powders have been described which may differ somewhat in their dispersibility in a plastic binder solution, but which otherwise might be expected to exhibit physical properties in tape form similar to the existing oxide tapes. Conventional acicular iron oxide particle tapes are compared next with the higher coercivity cobalt-doped iron oxide and with an alloy powder tape. All three tapes have similar total magnetic fluxes and, as a result, the alloy powder has a thickness about one-third that of the oxide tapes. It was indicated in the discussion of tape design criteria that a reduction of the magnetic coating thickness would lead to higher resolution for all practical forms of recording.

Static Magnetization Characteristics

As described, some guide to the recording resolution, stability, and reproduced output capability can be obtained by comparing the remanent magnetization characteristics of tapes. In Fig. 4, the reduced remanent magnetization curves are plotted for two oriented acicular particle tapes, curves (b) and (c), and one non-oriented spherical particle tape, curve (a). It can be seen that the desirable steep and linear rise is best obtained in the iron oxide tape. This is attributed to a higher degree of particle orientation and a reduced spread of particle switching fields compared to the alloy powder tape. Similarly, the uniformity of effective switching fields is also inferior in the crystal anisotropy controlled spherical particles.

The ac bias recording performance is related to the anhysteretic magnetization characteristic which is plotted for the three powders in Fig. 5. The greater influence of internal fields in the spherical particle cobalt-doped iron oxide is responsible for its lower initial anhysteretic susceptibility. The oriented acicular particle tapes have inherently more linear anhysteretic characteristics. Again the superior orientation of the iron oxide tape results in the better characteristic.

Frequency Response and Noise Level

The most important characteristic distinguishing one tape from another is short wavelength response. However, the wavelength dependence of the recorded flux is extremely difficult to measure accurately, because of uncertainty of the losses in the reproducing process. Reproducing heads have wavelength-dependent losses because of the finite length of the gap and imperfect

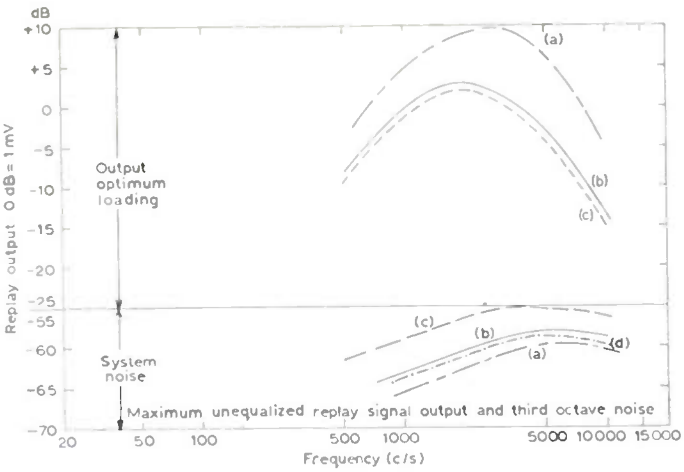

Fig. 6—Comparison of magnetic powder tapes.

contact between tape and head. Frequency-dependent losses also occur because of eddy currents in the head core, but these may be kept negligible by testing tapes at very slow speeds rather than at high frequencies. The technique for making ultrafine gap reproducing heads has so progressed that head sensitivity may be held within a few decibels for reproduction of wavelengths down to about 4 μ. Thus, comparison of frequency response and output capability is possible if high-precision recording and reproducing heads are used.

The recording performances of four different magnetic powder tapes are compared in Fig. 6 (upper set of curves) where the maximum reproducing-head output is shown as a function of frequency, using a slow tape speed of $1\frac{7}{8}$ inches per sec. Curves are drawn for a thin layer tape of alloy powder, and for thicker layers of oxide powder tapes having comparable remanent fluxes and, hence, comparable long-wavelength responses. These curves include two acicular particle tapes having different particle sizes, and a small-size nonacicular particle tape. The curves correspond to a harmonic distortion level of 5 per cent or less. Since the output curves depend in a complicated way on the bias amplitude, this is chosen as a compromise between overbiasing the short wavelengths and underbiasing the long ones and is a function of the field gradient through the thickness of the coating. A better compromise bias is achieved in thinner coatings. In the curves shown, the bias is optimized for the mid-frequency range, and it is clearly seen that the thin layer of high-magnetization alloy powder is superior in over-all output. This is caused by variations of bias level through the coating minimizing the loss.

The effect of particle size on the zero-modulation noise may also be seen in Fig. 6 (lower set of curves). Here the noise, measured in third-octave bands, is plotted for the four tapes. The superiority of the alloy powder, with its extremely small particle size, again is evident. Thus, in ac bias recording, the predicted improved performance from a thin high-remanent magnetization material is demonstrated. If such layers can be produced with sufficient physical uniformity and stability, improved tapes using such materials would appear to be forthcoming.

Conclusions

Design criteria for improved magnetic tapes demand for the present techniques of recording and reproduction that the magnetic layer thickness be reduced as much as possible. At present, oxide powders offer a good compromise to the optimum magnetic properties required. When techniques for preparing physically satisfactory thin films become available, it is to be expected that metallic magnetic layers, either in powder form or directly deposited, will become the preferred material.

References

[1] D. W. Chapman, "Optimizing the digital magnetic recording process," Proc. IEEE (*Correspondence*), pp. 247–248; January, 1963.

[2] K. Teer, "Investigation of the magnetic recording process with step functions," *Philips Research Reports*, vol. 16, pp. 469–491; October, 1961.

[3] R. L. Price, "Modulation noise in magnetic tape recordings," IRE Trans. on Audio, vol. AU-6, pp. 29–40; March–April, 1958.

[4] D. F. Eldridge, "DC and modulation noise in magnetic tape," IEEE Trans. on Communication and Electronics, vol. CE-83; 1964 (to be published).

[5] D. G. Tonge and E. P. Wohlfarth, "The remanent magnetization of single domain ferromagnetic particles," *Philosophical Magazine*, vol. 2, pp. 1333–1344; November, 1957.

[6] C. P. Bean, "Hysteresis loops of mixtures of ferromagnetic micro-powders," *J. Appl. Phys.*, vol. 26, pp. 1381–1383; November, 1955.

[7] M. Camras, "Magnetic materials and method of making magnetic material," U. S. Patent no. 2,694,656; November, 1954.

[8] W. P. Osmond, "An interpretation of the magnetic properties of some iron-oxide powders," *Proc. Phys. Soc.* (London), vol. 65B, pp. 121–133; February, 1952.

[9] —— "An interpretation of the magnetic properties of some iron-oxide powders—II," *Proc. Phys. Soc.* (London), vol. 66B, pp. 265–272; April, 1953.

[10] J. Smit and H. P. J. Wijn, "Ferrites," John Wiley and Sons, Inc., New York, N. Y., pp. 157, 194, 208; 1959.

[11] Société d'Ugine, "Improvements in or relating to the manufacture of magnets," U. K. Patent no. 596,875; 1948.

[12] A. H. Mones and E. Banks, "Cation substitutes in $BaFe_{12}O_{19}$," *J. Phys. Chem. Solids*, vol. 4, pp. 217–222; January-March, 1958.

[13] H. Kojima, "Effects of additionals on the magnetic properties of P_bO-$E_{E_2}O_3$ System," *Science Reports* (Japan), vol. 8, pp. 540–546; December, 1956.

[14] J. N. Ingraham and T. J. Swoboda, "Antimony-modified chromium oxide ferromagnetic compositions, their preparation and use," U. S. Patent no. 2,923,683; 1960.

[15] A. E. Berkowitz and W. J. Schuele, "Magnetic properties of some ferrite micropowders," *J. Appl. Phys. Suppl.*, vol. 30, pp. 134S–135S; April, 1959.

[16] F. Krones, "Technik Der Magnetspeicher," Springer-Verlag, Berlin, Germany, p. 425; 1960.

[17] Agfa, "Magnetizable metal oxides," U. K. Patent no. 717,269; 1954.

[18] J. C. Jeschke, "Magnetogrammtrager," East German Patent no. 8,681; 1954.

[19] Y. Sugiura, "Magnetic anisotropy of iron-cobalt ferrite measured by ferromagnetic resonance," *Journal*, Physical Society of Japan, vol. 15, pp. 360–373; August, 1960.

[20] C. D. Mee and J. C. Jeschke, "Single domain properties in hexagonal ferrites," *J. Appl. Phys.*, vol. 34, pp. 1271–1272; April, 1963.

[21] H. B. G. Casimir, J. Smit, U. Enz, J. F. Fast, H. P. J. Wijn, E. W. Gorter, J. D. Fast, A. J. W. Duyvesteyn, and J. J. DeJong, "Rapport sur quelques recherche dans la domain du magnetisme aux laboratoires Philips," *J. Phys. Radium*, vol. 20, pp. 360–373; February–March, 1959.

[22] G. H. Jonker, H. P. J. Wijn, and P. B. Braun, "A new class of oxidic ferromagnetic materials with hexagonal crystal structures," *Proc. IEE*, vol. 104B, suppl. 5–7, pp. 249–265; 1957.

[23] A. L. Stuijts and H. P. J. Wijn, "Crystal-oriented ferroxplana,"

Philips Tech. Rev., vol. 19, pp. 209–217; December, 1958.

[24] H. Kojima, "Effects of some additionals for the magnetic properties of B_A and S_R oxide magnets," *Science Reports*, vol. 10, pp. 175–182; 1958.

[25] T. J. Swoboda, P. Arthur, Jr., N. L. Cox, J. N. Ingraham, A. L. Oppegard, and M. S. Sadler, "Synthesis and properties of ferromagnetic chromium oxide," *J. Appl. Phys.*, vol. 32, pp. 274S–275S; March, 1961.

[26] F. G. Luborsky, L. I. Mendelsohn, and T. O. Paine, "Reproducing the properties of alnico permanent magnetic alloys with elongated single-domain cobalt-iron particles," *J. Appl. Phys.*, vol. 28, pp. 344–351; March, 1957.

[27] R. M. Bozorth, "Some magnetic electrical and optical properties of electrolytic and evaporated films," *J. Phys. Radium*, vol. 17, pp. 256–262; March, 1965.

[28] W. H. Meiklejohn, "Experimental study of the coercive force of fine particles," *Rev. Mod. Phys.*, vol. 25, pp. 302–306; January, 1953.

[29] J. S. Sallo and J. M. Carr, "Studies of high-coercivity cobalt-phosphorus electrodeposits," *J. Appl. Phys.*, vol. 33, pp. 1316–1317; March, 1962.

[30] T. H. Bonn and B. E. Wendell, Jr., "Electrodeposition of a magnetic coating," U. S. Patent no. 2,644,787; July, 1953.

[31] S. Iwasaki and K. Nagai, "Some consideration on the design of high output magnetic tape for short wavelength recording," *Proc. Magnetic Recording Conf.*, Budapest, Hungary, 1962.

[32] P. T. Hobson, E. S. Chatt, and W. P. Osmond, "A magnetic study of stainless steel wires," *J. Iron Steel Inst.* (London), vol. 159, pp. 145–157; June, 1948.

[33] E. M. Underhill, "Permanent magnet alloys," *Electronics*, vol. 21, p. 122; January, 1948.

[34] F. E. Luborsky, T. O. Paine, and L. I. Mendelsohn, "Permanent magnets from elongated single-domain particles," *Powder Met. Bull.*, vol. 4, pp. 57–78; 1959.

[35] W. J. Schuele, "Preparation of fine particles from bimetal oxalates," *J. Phys. Chem.*, vol. 63, pp. 83–86; January, 1959.

[36] Société d'Ugine, "Improvements in or relating to the manufacture of magnets," U. K. Patent no. 590,392; 1947.

[37] K. Nagai, *et al.*, "Some reports on powdered alloy magnetic tape-II," *Proc. Joint Meeting Electrical Inst.*, no. 734, pp. 1–2; April, 1959.

[38] I. Tsu, "A new cobalt-nickel sulfamate bath," *Plating*, vol. 48, pp. 379–381; April, 1961.

[39] J. S. Sallo and K. H. Olsen, "Studies of a high-coercivity electrodeposit having a lamellar structure," *J. Appl. Phys.*, vol. 32, p. 203S; March, 1961.

[40] G. Bate and D. Speliotis, "Hard magnetic films of Co-Ni-P," *J. Appl. Phys.*, vol. 34, pp. 1073–1074; April, 1963.

[41] R. D. Fisher and W. H. Chilton, "Preparation and magnetic characteristics of chemically deposited cobalt for high-density storage," *J. Electrochem. Soc.*, vol. 109, pp. 485–490; June, 1962.

[42] M. S. Blois, Jr., "Preparation of thin magnetic films and their properties," *J. Appl. Phys.*, vol. 26, pp. 975–980; August, 1955.

[43] A. Dupre, "Electrical and magnetic properties of thin cobalt films," *Cobalt*, pp. 1–5; March, 1960.

[44] H. Koretzky, "Electrodeposited magnetic films—a critical survey," *Proc. First Australian Conf. on Electrochemistry*, pp. 417–433; 1964.

Contributors

Warren R. Kundert (S'54–M'59) was born in Boston, Mass. on January 17, 1936. He received the B.S.E.E degree in 1958 and the M.S.E.E. degree in 1961 from Northeastern University, Boston, Mass.

He joined General Radio Company, Concord, Mass. in 1959 where he has been engaged in developing apparatus for measuring sound and vibration.

Mr. Kundert is a member of Eta Kappa Nu and the Acoustical Society of America.

Charles D. Mee (SM'58) was born in Loughborough, England, on December 28, 1927. He received the B.Sc. degree in physics from London University, England, in 1948 and the Ph.D. degree from Nottingham University, England, in 1951.

From 1951 to 1954, he was employed by the Magnetic Laboratory of the Steel Company of Wales, Newport, England, where he specialized in research on soft magnetic materials. Then he became associated with the MSS Recording Company, Colnbrook, England, where he was in charge of a research program on the development of data recording magnetic tape. In 1957 he joined CBS Laboratories, Stamford, Connecticut, where he directed research programs on short wavelength magnetic recording problems, video recording and new magnetic materials for tape. In 1962 he joined the IBM Research Center, Yorktown Heights, N. Y. where he is Manager of the Exploratory Magnetic Devices Group.

Dr. Mee is a member of the Institute of Physics.

Donald E. Richardson (SM'30–F'50) was born in Farina, Ill., on April 12, 1899. He received the B.S. degree in electrical engineering from Armour Institute of Technology (presently Illinois Institute of Technology), Chicago, Ill., and in 1924, the M.S. degree in physics from the University of Chicago, Chicago, Ill., in 1929.

Prior to his retirement in August of 1964, he was a Senior Engineer in the Electronics Research Division of ITT Research Institute.

Mr. Richardson is a member of the American Association for the Advancement of Science, the American Physical Society, the American Society for Engineering Education, the society of American Military Engineers, Sigma Xi, Tau Beta Pi, Eta Kappa Nu, and Sigma Pi Sigma.

Henry Seiwatz was born in New York, N. Y., on January 27, 1931. He received the B.A. and M.S. degrees in physics from Cornell University, Ithaca, N. Y., in 1952 and 1955, respectively, he did graduate work in biophysics as an N.S.F. Fellow at Yale University, New Haven, Conn., from 1954 to 1956.

He has been a member of the Physics Research Division of IIT Research Institute, Chicago, Ill., since 1956, where he is presently a Research Physicist in the Solid State Physics Section.

Mr. Seiwatz is a member of the American Physical Society.

Information for Contributors

Readers are encouraged to submit manuscripts, guest editorials, news items and letters. All material should be sent to Peter W. Tappan, Editor, IEEE Transactions on Audio, Bolt Beranek and Newman Inc., 1740 Ogden Avenue, Downers Grove, Ill.

All typed material should be double spaced with wide margins on one side of $8\frac{1}{2} \times 11$ inch paper. A carbon or other copy should be included if possible. All material should be mailed flat, not rolled into a tube.

Submission of material is a representation that it has not been copyrighted, published, submitted for publication or presented elsewhere unless explicit notice to the contrary is given.

Illustrations

All illustrations or figures should be $8\frac{1}{2} \times 11$ inches or smaller and should not be folded. Any illustration which is smaller than 8×10 inches should be attached to an $8\frac{1}{2} \times 11$ inch piece of paper. Photographs should be on glossy paper. Drawings and graphs should be in black ink on white paper (or on tracing cloth or tracing paper). Divisions on ordinary graph paper are too close together to reproduce well, and graphs should be traced or drawn on white paper, showing only the major intersecting grid lines. In circuit diagrams, each junction of wires should be indicated with a bold dot. Nonconnecting crossovers should be avoided where feasible, and should be indicated with a semicircular bridge or "wicket." In a schematic diagram of an actual circuit, component values should be shown on the diagram where feasible. A separate ground symbol for each ground connection is preferable to a single ground bus.

Each figure and table should have a caption that will be intelligible to the reader without consulting the text, if possible. A complete list of figure captions on a separate page should be included with each manuscript.

Manuscripts

The author's name should appear at the top of each page of his manuscript and on each figure. A 200-word or shorter abstract of the paper should precede the text.

The author should take special care to make all mathematical expressions clear to the printer. Greek letters and unusual symbols should be spelled out in the margin. Only the simplest formulas should be typewritten; all others should be carefully printed in ink. Do not give derivations that are easily found in the literature; merely cite the reference.

References and/or footnotes should appear as consecutively numbered in text. They should be listed on a separate page at the end of the manuscript. Book references should contain the author's initials and name, book title, publisher, city of publication, the page or pages referred to and the year of publication. Periodical references should contain the author's initials and name, title of the article or paper, name of the publication, volume number, page numbers, month or months and year.

INSTITUTIONAL LISTINGS

The IEEE Audio Group is grateful for the assistance given by the firms listed below, and invites application for Institutional Listing from other firms interested in Audio Technology.

Charge for listing in six consecutive issues of the TRANSACTIONS—$75.00.
Application for listing may be made to R. M. Emberson, Groups Secretary,
The Institute of Electrical and Electronics Engineers, Inc.,
345 East 47 Street, N.Y. 10017